Analysis of the Shear Lag Factor for Slotted Rectangular HSS Members

BO DOWSWELL

ABSTRACT

Rectangular HSS tension members are often connected by slotting two opposite walls and welding the slotted walls to a gusset plate. Due to a nonuniform stress distribution in these connections, the tensile rupture strength of the member is dependent on a shear lag factor. The accuracy of the 2016 AISC *Specification* provisions for the tensile rupture strength of slotted HSS tension members was evaluated using existing data from five previous research projects. The results revealed that the current equations are excessively conservative. The accuracy can be improved by replacing the existing equation for the connection eccentricity with the equation proposed in this paper.

Keywords: shear lag factor, HSS, gusset plate, tensile rupture, nonuniform stress distribution.

INTRODUCTION

Rectangular hollow structural sections (HSS) are often used as vertical bracing members in steel structures. A common connection detail for these members is shown in Figure 1, where two opposite walls are slotted to allow the brace to be inserted over the gusset plate. The brace is then connected to the gusset plate with four fillet welds.

A nonuniform stress distribution exists at the connection, which can reduce the tensile rupture strength of the member. This effect is addressed in the 2016 AISC *Specification for Structural Steel Buildings* (AISC, 2016), hereafter referred to as the AISC *Specification*, with a shear lag factor, U. For conditions where some cross-sectional elements are unconnected, the AISC *Specification* equation (Equation 3) was empirically derived using experimental results on open structural shapes (Chesson and Munse, 1963). However, the reliability of this equation has not been documented for slotted rectangular HSS connections. The objective of this paper is to analyze the existing data from previous research projects to determine the accuracy of the AISC *Specification* provisions for these connections.

TENSILE RUPTURE STRENGTH

AISC *Specification* Section D2 defines the nominal tensile rupture strength as

$$P_n = F_u A_e \qquad (Spec.\ \text{Eq. D2-2})$$

Bo Dowswell, PE, PhD, ARC International, LLC, Birmingham, Ala. Email: bo@arcstructural.com

Paper No. 2020-03

where $\phi = 0.75$ (LRFD), $\Omega = 1.67$ (ASD), F_u is the specified minimum tensile strength of the HSS, and A_e is the effective net area, which is defined in AISC *Specification* Section D3 as

$$A_e = A_n U \qquad (Spec.\ \text{Eq. D3-1})$$

where A_n is the net area, calculated by subtracting the slot area from the gross area according to Equation 1:

$$A_n = A_g - 2tw_s \tag{1}$$

where t is the HSS wall thickness and w_s is the slot width, as shown in Figure 2.

The gross area, calculated with Equation 2, is based on a corner radius equal to twice the wall thickness. Equation 2 was used to calculate the areas listed in AISC *Steel Consstruction Manual* (AISC, 2017) Tables 1-11 and 1-12.

$$A_g = 2t(H+B) + t^2(3\pi - 16) \tag{2}$$

where B is the width of the HSS member perpendicular to the gusset plate and H is the width of the HSS member parallel to the gusset plate. Case 6 in AISC *Specification* Table D3.1 corresponds to slotted rectangular HSS members, where the shear lag factor, U, is defined with Equation 3.

$$U = 1 - \frac{\bar{x}}{l} \tag{3}$$

where l is the connection length. For the 2016 AISC *Specification*, l must be greater than H.

The connection eccentricity, $\bar{x}$, calculated with Equation 4, is the distance from the center of the gusset plate to the centroid of the C-shaped portion of the HSS on each side of the gusset plate. Equation 4 is conservative because the derivation was based on the outside HSS dimensions, while neglecting the gusset plate thickness.

$$\bar{x} = \frac{B^2 + 2BH}{4(B+H)} \tag{4}$$

The accuracy can be improved by defining $\bar{x}$ as the distance from the edge of the gusset plate to the centroid of the C-shaped portion of the HSS on each side of the gusset plate. In this case, $\bar{x}$ is calculated with Equation 5, which is less conservative than Equation 4 because both the HSS wall thickness and the gusset plate thickness were considered in the derivation.

$$\bar{x} = b - \frac{2b^2 + Ht - 2t^2}{2H + 4b - 4t} \tag{5}$$

where b is the distance from the HSS outer surface to the gusset edge as shown in Figure 2.

$$b = \frac{B - t_g}{2} \tag{6}$$

DATA ANALYSIS

Existing Data

Slotted rectangular HSS connections have been studied using both finite element models (Girard et al., 1995; Zhao et al., 2009) and experimental specimens. As noted by Martinez-Saucedo and Packer (2007), many of the available experimental specimens failed by either block shear rupture (Zhao et al., 1999; Zhao and Hancock, 1995) or weld rupture (Wilkinson et al., 2002), not circumferential rupture, which is indicative of a tension rupture failure. Due to inconsistent results from the finite element models, the data for this study includes only the experimental specimens that failed by circumferential rupture at the connection.

A total of 47 specimens from five research projects were analyzed. All specimens were connected by four longitudinal fillet welds as shown in Figure 1. For the 10 specimens tested by Yeomans (1993), additional transverse welds connected the HSS walls to the edge of the gusset plates. The geometric and material variables for the test specimens are listed in columns 2 through 8 of Table 1, and the experimental rupture load, P_e, is listed in column 9. The specimens tested by Zhao et al. (2008), Korol et al. (1994), and Yeomans (1993) were loaded statically, and the specimens tested by Han et al. (2007) and Yang and Mahin (2005) were loaded cyclically to simulate seismic loading.

Using the measured dimensions and tensile strengths (where available), the tension rupture strength, P_c, was calculated for each specimen. For the 10 specimens tested by Yeomans (1993), the transverse welds were considered in the calculations by setting the net area equal to the gross area. The strengths, with $\bar{x}$ calculated with Equations 4 and 5 are listed in columns 5 and 6 of Table 2, respectively.

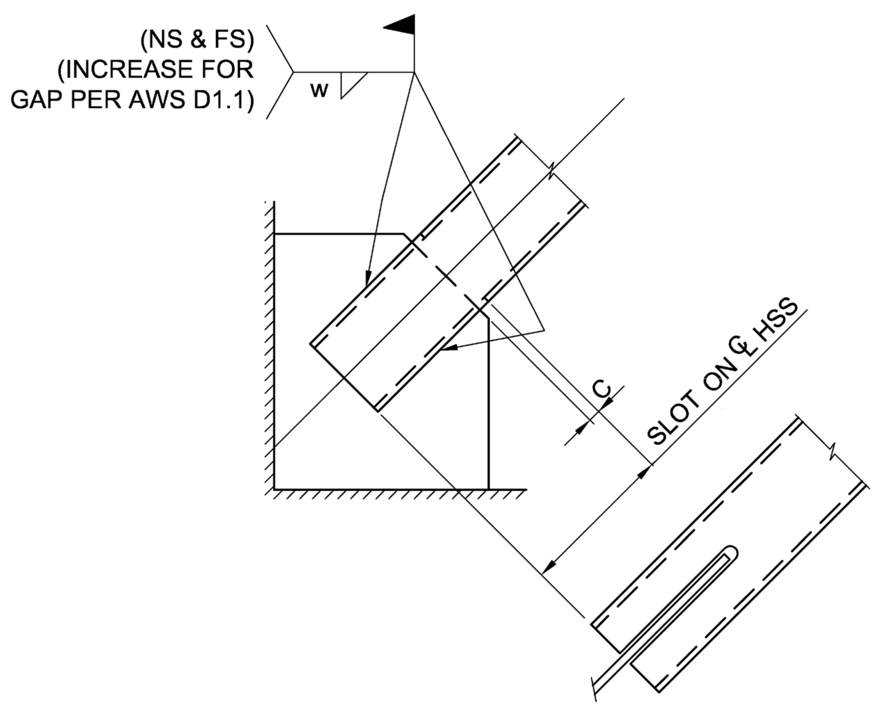

Fig. 1. Slotted rectangular HSS brace connection.

The measured tensile strength, σ_u, was not reported for the specimens tested by Korol et al. (1994); therefore, the calculated strength was based on the specified minimum tensile strength, F_u. The experimental-to-calculated load ratios, P_e/P_c, are listed in columns 7 and 8.

Reliability Analysis

The reduction factor required to obtain a specific reliability level is (Galambos and Ravinda, 1978):

$$\phi = C\rho_R e^{-\beta\alpha_R V_R} \tag{7}$$

where

C = correction factor

V_R = coefficient of variation

α_R = separation factor

β = reliability index

ρ_R = bias coefficient

Based on AISC *Specification* Section B3.1 Commentary, the target reliability index used in this paper is 4.0. Galambos and Ravinda (1973) proposed a separation factor, α_R, of 0.55. For a live-to-dead load ratio, L/D, of 3.0, Grondin et al. (2007) developed Equation 8 for calculating the correction factor.

$$C = 1.4056 - 0.1584\beta + 0.008\beta^2 \tag{8}$$

The bias coefficient is

$$\rho_R = \rho_M \rho_G \rho_P \tag{9}$$

where

ρ_G = bias coefficient for the geometric properties

ρ_M = bias coefficient for the material properties

ρ_P = bias coefficient for the test-to-predicted strength ratios. Mean value of the professional factor calculated with the measured geometric and material properties

The coefficient of variation is

$$V_R = \sqrt{V_M^2 + V_G^2 + V_P^2} \tag{10}$$

where

V_G = coefficient of variation for the geometric properties

V_M = coefficient of variation for the material properties

V_P = coefficient of variation for the test-to-predicted strength ratios

The relevant geometric parameters for slotted HSS connections are the wall thickness and weld length. Wall thickness measurements for the 30 ASTM A500 Grade C specimens tested by Zhao et al. (2008) resulted in a mean measured-to-nominal thickness ratio of 0.924. Using a design wall thickness equal to 0.93 times the nominal wall thickness according to AISC *Specification* Section B4.2, the mean measured-to-design thickness ratio is 0.994, with a coefficient of variation of 0.00710.

To the author's knowledge, the required statistical information on weld length is not available. For the block shear limit state of slotted HSS connections, Oosterhof and Driver (2011) used ρ_G = 1.00 and V_G = 0.050. These values were originally used by Hardash and Bjorhovde (1984) for bolted gusset plates, and they were "assumed to be appropriate in the absence of better statistical data" for slotted HSS connections. Because the same parameters are relevant for the tensile rupture limit state, V_G = 0.050 was used for the analysis in this paper. The slightly more conservative value of ρ_G = 0.994, which was based on the wall thickness measurements by Zhao et al. (2008), was used in the analysis.

Statistical values for the tensile strength of as-formed rectangular HSS shapes, summarized by Schmidt and Bartlett (2002), are ρ_M = 1.18 and V_M = 0.063. A more recent data set compiled by Liu et al. (2007) resulted in ρ_M = 1.27 and V_M = 0.04 based on 309 specimens from rectangular ASTM A500 Grade B shapes.

For five of the projects discussed in this paper (Zhao et al., 2008; Han et al., 2007; Yang and Mahin, 2005; Zhao et al., 1999; Zhao and Hancock, 1995), 20 data points are available with coupons extracted from the flat portions of the HSS walls. These tests—on ASTM A500 Grade B, ASTM A500 Grade C, and similar international grades—resulted in ρ_M = 1.12 and V_M = 0.0405, with only a small variation between grades.

Three tension specimens were extracted from the HSS corners and tested by Zhao et al. (2008). Due to the cold-bending of the corners, the tensile strength at the corners was 23% higher than the tensile strength at the flat portions of the walls.

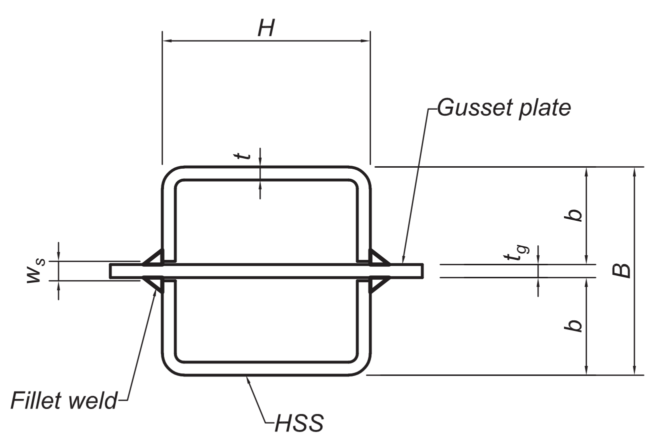

Fig. 2. HSS section at slot.

Results

Conservative values for the geometric and material properties are $\rho_G = 0.994$, $V_G = 0.050$, $\rho_M = 1.12$, and $V_M = 0.063$. These values were used to analyze two data sets: (1) the 36 specimens tested by Zhao et al. (2008) and Yeomans (1993) and (2) all 47 specimens listed in Table 1.

The rupture strengths calculated with Equation 4 varied from 0.865 to 0.968 times the values calculated with Equation 5, with an average of 0.935. Because Equation 4 is more conservative than Equation 5, only Equation 5 was used in the analysis.

For the 36 specimens tested by Zhao et al. (2008) and Yeomans (1993), the average test-to-predicted strength ratio, ρ_P, is 1.26 with a coefficient of variation, V_P, of 0.0872. Substituting these values into Equations 9 and 10 results in $\rho_R = 1.40$ and $V_R = 0.119$. Using Equations 7 and 8, $\phi = 0.970$ at $\beta = 4.0$ and $\beta = 5.57$ at $\phi = 0.75$.

Because the measured tensile strength, σ_u, was not reported for the specimens tested by Korol et al. (1994), the experimental-to-calculated load ratio, P_e/P_c, for these specimens was divided by ρ_M prior to the calculation of ρ_P. For all 47 specimens, $\rho_P = 1.22$, $V_P = 0.104$, $\rho_R = 1.36$, and $V_R = 0.132$. Using Equations 7 and 8, $\phi = 0.916$ at $\beta = 4.0$ and $\beta = 5.15$ at $\phi = 0.75$.

The analysis showed that the reliability index, with $\bar{x}$ calculated using Equation 5, is greater than the target reliability index of 4.0. Therefore, $\phi = 0.75$ is conservative. At least a portion of this conservatism can be attributed to the increase in tensile strength at the corners that is caused by cold-working.

Discussion

For the 2016 AISC *Specification*, l must be greater than H. This requirement evolved from the 1986 AISC *Specification* (AISC, 1986) limit that was initially applicable only to plates with longitudinal welds along both edges. In the 2016

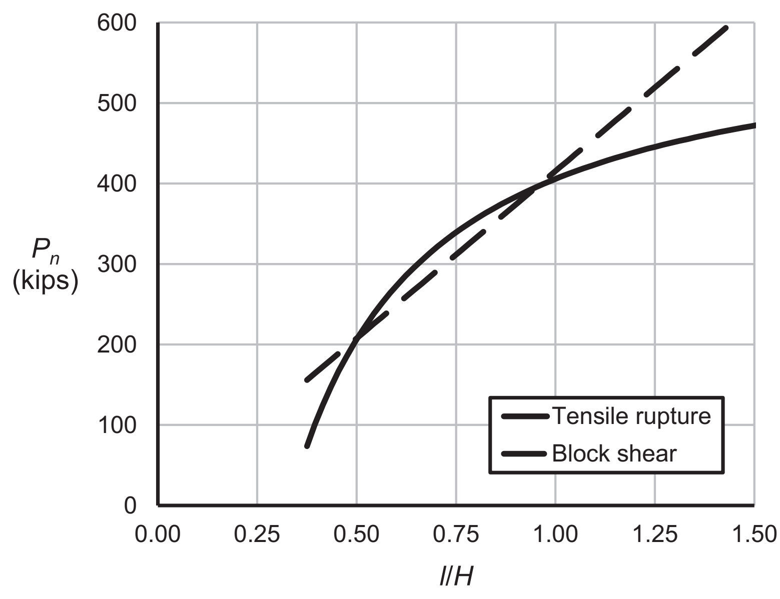

Fig. 3. Nominal strength of a slotted HSS8×8×⅜ connection vs. length-to-height ratio.

Specification provisions, this limit is not required for plates with longitudinal welds.

Column 10 in Table 1 shows only one specimen with an l/H ratio less than 1.0. For Zhao et al. (2008) specimen RS3G05P16, l/H = 0.924 and the experimental-to-calculated strength ratio, P_e/P_c = 1.24 with $\bar{x}$ calculated using Equation 5. However, only the specimens that failed by circumferential rupture at the net section were included in Table 1.

Figure 3 shows the variation in nominal strength with the l/H ratio for a slotted HSS8×8×⅜ connection of ASTM A500 Grade C material. In this case, the strength is controlled by the block shear limit state for $0.504 < l/H < 0.951$, and the tensile rupture limit state controls the strength for other l/H ratios. The curves for rectangular HSS with $H/B >$ 1.0 are similar to the curve for square HSS in Figure 3. For example, for an HSS12×4×⅜, the strength is controlled by the block shear limit state for $0.125 < l/H < 0.845$. For some conditions with $H/B < 1$, the tensile rupture strength is always lower than the block shear strength, potentially leading to uneconomical designs when both $H/B < 0.50$ and $l/H < 1.0$.

The 72 slotted HSS specimens that were tested by Zhao et al. (1999) and Zhao and Hancock (1995) failed by block shear. For these specimens, the l/H ratios were between 0.533 and 1.10, and most of the specimens had $l/H < 1.0$. Oosterhof and Driver (2011) showed that the 2016 AISC *Specification* equations for block shear are appropriate but slightly conservative for calculating the strength of these specimens.

Column 11 in Table 1 shows that the specimens had aspect ratios in the range $0.40 \le B/H \le 2.5$. Figure 4 shows the variation in the test-to-predicted strength ratio, P_e/P_c, with the B/H ratio. Although the conservatism of the proposed design equations is generally higher for the four specimens with $B/H \approx 2.5$ compared to the total data set, a significant trend cannot be established using the existing data.

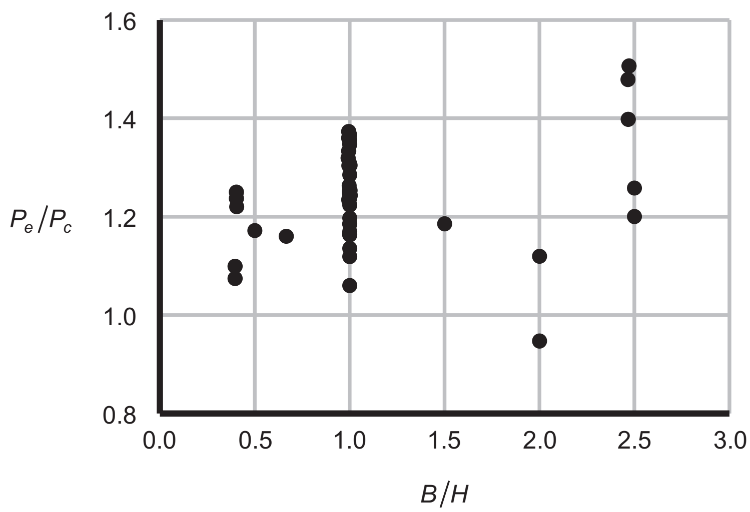

Fig. 4. Test-to-predicted strength ratio vs. width-to-height ratio.

Table 1. Specimen Details											
Specimen	B in.	H in.	t in.	l in.	t_g in.	F_u ksi	σ_u ksi	P_e kips	l/H	B/H	Notes
Zhao et al. (2008)											
RL5G05P16	5.01	2.03	0.176	7.69	0.619	62	65.0	152	3.79	2.47	
RS5G05P16	2.02	5.01	0.176	7.68	0.620	62	65.0	152	1.53	0.404	
SM5G05P16	3.53	3.53	0.174	7.67	0.619	62	70.3	153	2.17	1.00	
SM5G05P16R	3.52	3.53	0.174	7.75	0.620	62	70.3	151	2.20	1.00	
RL4G05P16	5.01	2.03	0.176	6.12	0.620	62	65.0	152	3.01	2.47	
RS4G05P16	2.03	5.01	0.177	6.13	0.621	62	65.0	147	1.22	0.405	
SM4G05P16	3.52	3.53	0.173	6.15	0.621	62	70.3	152	1.74	1.00	
SM4G05P16R	3.53	3.52	0.174	6.19	0.621	62	70.3	152	1.76	1.00	
RL3G05P16	5.00	2.02	0.176	4.55	0.618	62	65.0	138	2.25	2.47	
RS3G05P16	2.02	5.01	0.178	4.63	0.626	62	65.0	144	0.924	0.404	
SM3G05P16	3.53	3.53	0.174	4.54	0.614	62	70.3	146	1.29	1.00	
SM3G05P16R	3.52	3.52	0.174	4.56	0.619	62	70.3	147	1.29	1.00	
SM3G05P12	3.52	3.52	0.174	4.70	0.498	62	70.3	152	1.33	1.00	
SM3G05P12R	3.52	3.52	0.174	4.64	0.500	62	70.3	150	1.32	1.00	
SM5G05P12	3.53	3.52	0.174	7.93	0.501	62	70.3	156	2.25	1.00	
SM5G05P12R	3.54	3.53	0.174	7.93	0.499	62	70.3	155	2.25	1.00	
SM3G05P20	3.50	3.50	0.174	4.50	0.754	62	70.3	140	1.29	1.00	
SM3G05P20R	3.52	3.55	0.175	4.48	0.752	62	70.3	143	1.26	0.992	
SM5G05P20	3.53	3.53	0.174	7.50	0.755	62	70.3	150	2.13	1.00	
SM5G05P20R	3.52	3.53	0.174	7.48	0.754	62	70.3	152	2.12	1.00	
SM3G25P16	3.52	3.53	0.174	4.62	0.620	62	70.3	149	1.31	1.00	
SM3G25P16R	3.52	3.54	0.174	4.60	0.619	62	70.3	150	1.30	0.994	
SM3G50P16	3.51	3.53	0.174	4.59	0.618	62	70.3	150	1.30	0.995	
SM3G50P16R	3.51	3.53	0.174	4.56	0.617	62	70.3	146	1.29	0.995	
SM5G50P16	3.52	3.53	0.174	7.72	0.619	62	70.3	151	2.19	1.00	
SM5G50P16R	3.51	3.53	0.173	7.69	0.618	62	70.3	151	2.18	1.00	
Yeomans (1993)											
S-SEP-2	1.97	1.97	0.134	3.15	0.602	—	66.7	62	1.60	1.00	1
S-SEP-3	1.97	1.97	0.244	2.95	0.787	—	69.9	114	1.50	1.00	1
S-SEP-4	3.54	3.54	0.146	5.91	0.787	—	63.7	107	1.67	1.00	1
S-SEP-5	3.54	3.54	0.205	5.91	0.965	—	72.8	187	1.67	1.00	1
S-SEP-6	3.54	3.54	0.241	5.71	1.16	—	74.0	213	1.61	1.00	1
R-SEP-3	2.36	1.57	0.262	2.95	0.787	—	67.3	107	1.88	1.50	1
R-SEP-5	1.57	2.36	0.160	3.15	0.602	—	76.9	86	1.33	0.667	1
R-SEP-8	4.72	2.36	0.215	5.71	1.16	—	77.5	160	2.42	2.00	1
R-SEP-9	4.72	2.36	0.253	5.71	1.58	—	70.8	205	2.42	2.00	1
R-SEP-10	2.36	4.72	0.140	5.91	0.602	—	65.8	126	1.25	0.500	1

Table continues on the next page

Table 1. Specimen Details (continued)											
Specimen	***B*** **in.**	***H*** **in.**	***t*** **in.**	***l*** **in.**	t_g **in.**	F_u **ksi**	σ_u **ksi**	P_e **kips**	l/H	B/H	**Notes**
Korol et al. (1994)											
1A	4.92	1.97	0.252	6.30	0.630	65	—	168	3.20	2.50	2
1B	4.92	1.97	0.244	6.18	0.630	65	—	171	3.14	2.50	2
2A	3.46	3.46	0.242	6.18	0.630	65	—	164	1.78	1.00	2
2B	3.46	3.46	0.252	6.38	0.630	65	—	175	1.84	1.00	2
3A	1.97	4.96	0.242	6.14	0.630	65	—	174	1.24	0.397	2
3B	1.97	4.96	0.246	6.34	0.630	65	—	173	1.28	0.397	2
5A	3.50	3.50	0.236	3.86	0.630	65	—	149	1.10	1.00	2
Han et al. (2007)											
S90-8	3.94	3.94	0.354	9.88	0.669	58	66.1	293	2.51	1.00	3
S69-11	4.92	4.92	0.236	9.02	1.22	58	67.0	250	1.83	1.00	3
Yang and Mahin (2005)											
2	6.00	6.00	0.375	15.0	0.875	58	65.0	486	2.50	1.00	3
3	6.00	6.00	0.375	15.0	0.875	58	65.0	537	2.50	1.00	3

Note 1: Additional transverse welds connected the HSS walls to the edge of the gusset plates.
Note 2: The measured tensile strength, σ_u, was not reported.
Note 3: Cyclic loading was used to simulate seismic loading.

Table 2. Calculated Strengths							
		U		P_c**, kips**		P_e/P_c	
Specimen	A_n**, in.**^{2}	**Equation 4**	**Equation 5**	**Equation 4**	**Equation 5**	**Equation 4**	**Equation 5**
Zhao et al. (2008)							
RL5G05P16	2.03	0.790	0.821	104	109	1.45	1.40
RS5G05P16	2.01	0.887	0.928	116	121	1.31	1.25
SM5G05P16	2.02	0.827	0.862	118	122	1.30	1.25
SM5G05P16R	2.01	0.830	0.863	118	122	1.29	1.24
RL4G05P16	2.04	0.736	0.775	97.8	103	1.56	1.48
RS4G05P16	2.04	0.858	0.910	114	120	1.29	1.22
SM4G05P16	2.01	0.785	0.828	111	117	1.37	1.30
SM4G05P16R	1.99	0.786	0.829	110	116	1.37	1.30
RL3G05P16	2.03	0.646	0.698	85.1	91.9	1.63	1.51
RS3G05P16	2.04	0.813	0.881	108	117	1.34	1.24
SM3G05P16	2.02	0.708	0.766	100	109	1.46	1.35
SM3G05P16R	2.02	0.710	0.768	101	109	1.46	1.35
SM3G05P12	2.06	0.719	0.766	104	111	1.46	1.37
SM3G05P12R	2.07	0.715	0.763	104	111	1.45	1.36
SM5G05P12	2.06	0.833	0.861	121	125	1.30	1.25
SM5G05P12R	2.06	0.833	0.861	121	125	1.29	1.24
SM3G05P20	1.95	0.709	0.776	97.4	107	1.43	1.31

Table continues on the next page

Table 2. Calculated Strengths (continued)							
		U		P_c, kips		P_e/P_c	
Specimen	A_n, in.^{2}	**Equation 4**	**Equation 5**	**Equation 4**	**Equation 5**	**Equation 4**	**Equation 5**
Zhao et al. (2008) (continued)							
SM3G05P20R	1.99	0.705	0.773	98.6	108	1.45	1.32
SM5G05P20	1.97	0.824	0.864	114	120	1.31	1.25
SM5G05P20R	1.97	0.824	0.865	114	120	1.33	1.26
SM3G25P16	2.01	0.714	0.771	101	109	1.48	1.37
SM3G25P16R	2.02	0.713	0.770	101	109	1.48	1.37
SM3G50P16	2.03	0.713	0.770	102	110	1.47	1.36
SM3G50P16R	2.03	0.711	0.768	101	110	1.44	1.33
SM5G50P16	2.01	0.829	0.863	117	122	1.29	1.24
SM5G50P16R	2.01	0.828	0.862	117	122	1.28	1.23
Yeomans (1993)							
S-SEP-2	0.936	0.766	0.843	48	53	1.29	1.17
S-SEP-3	1.53	0.750	0.867	80	93	1.41	1.22
S-SEP-4	1.93	0.775	0.827	95	101	1.13	1.06
S-SEP-5	2.63	0.775	0.840	148	161	1.26	1.17
S-SEP-6	3.04	0.767	0.849	172	191	1.24	1.12
R-SEP-3	1.61	0.720	0.831	78	90	1.37	1.19
R-SEP-5	1.09	0.800	0.888	67	74	1.29	1.16
R-SEP-8	2.74	0.724	0.795	154	169	1.04	0.947
R-SEP-9	3.16	0.724	0.819	162	183	1.27	1.12
R-SEP-10	1.85	0.833	0.881	102	107	1.24	1.17
Korol et al. (1994)							
1A	2.72	0.749	0.791	133	140	1.27	1.20
1B	2.65	0.744	0.787	128	136	1.33	1.26
2A	2.65	0.790	0.837	136	144	1.20	1.14
2B	2.74	0.796	0.842	142	150	1.23	1.16
3A	2.65	0.863	0.919	149	159	1.17	1.10
3B	2.68	0.867	0.922	152	161	1.14	1.07
5A	2.63	0.659	0.734	113	126	1.32	1.19
Han et al. (2007)							
S90-8	4.22	0.851	0.885	238	247	1.23	1.19
S69-11	3.67	0.795	0.849	196	209	1.28	1.20
Yang and Mahin (2005)							
2	7.33	0.850	0.878	405	418	1.20	1.16
3	7.33	0.850	0.878	405	418	1.33	1.28

CONCLUSIONS

Rectangular HSS tension members are often connected by slotting two opposite walls and welding the slotted walls to a gusset plate. Due to nonuniform stress distributions in these connections, the tensile rupture strength of the member is dependent on a shear lag factor. The accuracy of the AISC *Specification* provisions for the tensile rupture strength of slotted HSS tension members was evaluated using existing data from previous research projects. A total of 47 specimens from five projects were analyzed.

The results revealed that the current equations are excessively conservative. The accuracy can be improved by replacing the 2016 AISC *Specification* equation (Equation 4) for the connection eccentricity, $\bar{x}$, with the proposed Equation 5, which is less conservative than Equation 4 because both the HSS wall thickness and the gusset plate thickness were considered in the derivation. The rupture strengths calculated with Equation 4 averaged 0.935 times the values calculated with Equation 5. Although the conservatism is reduced with the proposed Equation 5, the reliability analysis showed that the reduction factor, $\phi = 0.75$, in AISC *Specification* Section D2 is overly conservative when used with the proposed equation.

For practical connection geometries, the block shear limit state controls the strength of slotted HSS connections with low l/H ratios and the tensile rupture limit state controls the strength for high l/H ratios. If both limit states are checked, the connection rupture strength can be accurately predicted for the full range of available specimen geometries ($0.504 < l/H < 3.79$) without the 2016 AISC *Specification* requirement that l must be greater than H.

REFERENCES

AISC (1986), *Load and Resistance Factor Design Specification for Structural Steel Buildings*, American Institute of Steel Construction, Chicago, Ill.

AISC (2016), *Specification for Structural Steel Buildings*, ANSI/AISC 360-16, American Institute of Steel Construction, Chicago, Ill.

AISC (2017), *Steel Construction Manual*, 15th Ed., American Institute of Steel Construction, Chicago, Ill.

Chesson, E., Jr., and Munse, W.H. (1963), "Riveted and Bolted Joints: Truss Type Tensile Connections," *Journal of the Structural Division*, ASCE, Vol. 89, No. 1, January, pp. 67–106.

Galambos, T.V. and Ravinda, M.K. (1973), *Tentative Load and Resistance Factor Design Criteria for Steel Buildings*, Research Report No. 18, Department of Civil and Environmental Engineering, Washington University, September.

Galambos, T.V. and Ravinda, M.K. (1978), "Properties of Steel for Use in LRFD," *Journal of the Structural Division*, ASCE, Vol. 104, No. ST9, September, pp. 1,459–1,468.

Girard, C., Picard, A., and Fafard, M. (1995), "Finite Element Modelling of the Shear Lag Effects in an HSS Welded to a Gusset Plate," *Canadian Journal of Civil Engineering*, Vol. 22, pp. 651–659.

Grondin, G., Jin, M., and Josi, G. (2007), *Slip Critical Bolted Connections—A Reliability Analysis for Design at the Ultimate Limit State*, Structural Engineering Report No. 274, Department of Civil Engineering, University of Alberta, October.

Han, S.W., Kim, W.T., and Foutch, D.A. (2007), "Tensile Strength Equation for HSS Bracing Members Having Slotted End Connections," *Earthquake Engineering and Structural Dynamics*, Vol. 36, pp. 995–1,008.

Hardash, S.G. and Bjorhovde, R. (1984), *Gusset Plate Design Utilizing Block-Shear Concepts*, Department of Civil Engineering and Engineering Mechanics, University of Arizona, Tuscon, Ariz.

Korol, R.M., Mirza, F.A., and Mirza, M.Y. (1994), "Investigation of Shear-Lag in Slotted HSS Tension Members," *Tubular Structures VI*, Balkema, Rotterdam, pp. 473–479.

Liu, J., Sabelli, R., Brockenbrough, R.L., and Fraser, T.P. (2007), "Expected Yield Stress and Tensile Strength Ratios for Determination of Expected Member Capacity in the 2005 AISC *Seismic Provisions*," *Engineering Journal*, AISC, Vol. 44, No. 1, pp. 15–26.

Martinez-Saucedo, G. and Packer, J.A. (2007), "Discussion of Shear Lag in Rectangular Hollow Structural Section Tension Members: Comparison of Design Equations to Test Data," *Practice Periodical on Structural Design and Construction*, ASCE, Vol. 12, No. 2, pp. 135–136.

Oosterhof, S.A. and Driver, R.G. (2011), "Performance of the Unified Block Shear Equation for Common Types of Welded Steel Connections," *Engineering Journal*, AISC, Vol. 48, No. 2, pp. 77–92.

Schmidt, B.J. and Bartlett, F.M. (2002), "Review of Resistance Factor for Steel: Data Collection," *Canadian Journal of Civil Engineering*, Vol. 29, pp. 98–108.

Wilkinson, T., Petrovski, T., Bechara, E., and Rubal, M. (2002), "Experimental Investigation of Slot Lengths in RHS Bracing Members," *Proceedings of the 3rd International Conference on Advances in Steel Structures*, Elsevier, New York, N.Y., pp. 205–212.

Yang, F. and Mahin, S. (2005), "Limiting Net Section Fracture in Slotted Tube Braces," *Steel Tips*, Structural Steel Education Council, April.

Yeomans, N.F. (1993), *Slotted End Plate Connections*, TS and MD Technical Development Report No. P004.S.08-1, British Steel, March.

Zhao, R.G., Huang, R.F., Khoo, H.A., and Cheng, J.J.R. (2008), "Experimental Study on Rectangular and Square Hollow Structural Section (HSS) Tension Connections," *Canadian Journal of Civil Engineering*, Vol. 35, pp. 1,318–1,330.

Zhao, R.G., Huang, R.F., Khoo, H.A., and Cheng, J.J.R. (2009), "Parametric Finite Element Study on Slotted Rectangular and Square HSS Tension Connections," *Journal of Constructional Steel Research*, Vol. 65, pp. 611–621.

Zhao, X.L., Al-Mahaidi, R., and Kiew, K.P. (1999), "Longitudinal Fillet Welds in Thin-Walled C450 RHS Members," *Journal of Structural Engineering*, ASCE, Vol. 25, No. 8, August, pp. 821–828.

Zhao, X.L. and Hancock, G.J. (1995), "Longitudinal Fillet Welds in Thin Cold-Formed RHS Members," *Journal of Structural Engineering*, ASCE, Vol. 121, No. 11, November, pp. 1,683–1,690.